Properties of Stationary Nonequilibrium States in the Thermostatted Periodic Lorentz Gas II: The many point particles system

F. Bonetto†, D. Daems‡, J.L. Lebowitz*, V. Ricci⋆

Abstract: We study the stationary nonequilibrium states of N point particles moving under the influence of an electric field $\mathbf{E}$ among fixed obstacles (discs) in a two dimensional torus. The total kinetic energy of the system is kept constant through a Gaussian thermostat which produces a velocity dependent mean field interaction between the particles. The current and the particle distribution functions are obtained numerically and compared for small $|\mathbf{E}|$ with analytic solutions of a Boltzmann type equation obtained by treating the collisions with the obstacles as random independent scatterings. The agreement is surprisingly good for both small and large N. The latter system in turn agrees with a self consistent one particle evolution expected to hold in the $N \to \infty$ limit.

Keywords: Lorentz Gas, Gaussian Thermostat, Electrical Current, Steady state.

1. Introduction

In this note we continue our study of the stationary nonequilibrium states (SNS) of current carrying thermostatted systems. In part I [1] we described extensive numerical and analytical investigations of the dependence of the current on the electric field for a model single particle system introduced in [2] and previously studied in [3]. Here we study a generalization of that model to N particles introduced in [4]. The particles, which have unit mass, move among a fixed periodic array of discs in a two dimensional square Λ with periodic boundary conditions, see Fig. 1. They are acted on by an external (electric) field $\mathbf{E}$ parallel to the x-axis and by a "Gaussian thermostat". (The discs are located so that there is a finite horizon, *i.e.* there is a maximum distance a particle can move before hitting a disc or obstacle).

The equations of motion describing the time evolution of the positions $\mathbf{q}_i$ and velocities $\mathbf{v}_i, i = 1, ..., N$, are:

$$\begin{cases} \dot{\mathbf{q}}_i = \mathbf{v}_i \qquad \mathbf{q}_i = (q_{i,x}, q_{i,y}) \in \Lambda' \\ \dot{\mathbf{v}}_i = \mathbf{E} - \alpha(\mathbf{J}, U)\mathbf{v}_i + F_{obs}(\mathbf{q}_i) \end{cases} \tag{1.1}$$

where

$$\alpha(\mathbf{J}, U) = \frac{\mathbf{J} \cdot \mathbf{E}}{U}, \qquad \mathbf{J} = \frac{1}{N}\sum_{i=1}^{N} \mathbf{v}_i, \qquad U = \frac{1}{N}\sum_{i=1}^{N} \mathbf{v}_i^2 \tag{1.2}$$

Here $\Lambda' = \Lambda \backslash \mathcal{D}$, with $\mathcal{D}$ the region occupied by the discs (obstacles) and F_{obs} represents the elastic scattering which takes place at the surface of the obstacles. The purpose of the Gaussian thermostat, represented by the term $\alpha(\mathbf{J}, U)\mathbf{v}$ in eq.(1.1), is to maintain the total kinetic energy $1/2\sum_{i=1}^{N} \mathbf{v}_i^2$ constant, *i.e.* $U = v_0^2$. It also has the effect of making the flow Φ_t generated by eq.(1.1) on the $(4N-1)$ dimensional energy surface non Hamiltonian when $\mathbf{E} \neq 0$. In fact the phase space volume contraction rate is given by $\sigma(X) = -(2N-1)\alpha(\mathbf{J}, U)$. Another effect of the thermostat is to effectively couple all the particles in a mean field way, $\alpha(\mathbf{J}, U)$, depending

† School of Mathematics, Institute for Advanced Study, Princeton, NJ 08540. Email: bonetto@ias.edu

‡ Center for Nonlinear Phenomena and Complex Systems, Université Libre de Bruxelles, 1050 Brussels, Belgium. Email: ddaems@ulb.ac.be

* School of Mathematics, Institute for Advanced Study, Princeton, NJ 08540. Email: Lebowitz@math.rutgers.edu

⋆ Dipartimento di Matematica, Università "La Sapienza", Piazzale Aldo Moro n.5, 00185 Roma, Italy. Email: Valeria.Ricci@roma1.infn.it or ricci@mat.uniroma1.it

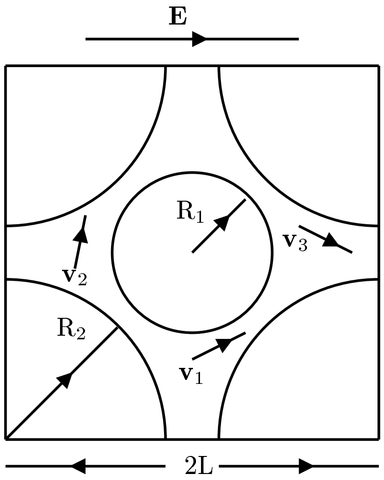

Fig. 1: General billiard structure with discs of radius R_1 and R_2 in a periodic box with side length $2L$, $N = 3$ particles are shown.

only on the total momentum of the particles. Note that this is the only coupling between the particles in this system.

The change of variables, $\mathbf{q}_i \to \mathbf{q}_i/L$, $\mathbf{v}_i \to \mathbf{v}_i/v_0$, $t \to tv_0/L$ and $\mathbf{E} \to \mathbf{E}L/v_0^2$, where $2L$ is the length of the box, leaves eq.(1.1) unchanged, so that the motion of the system takes place on $\mathcal{S}_N = (\Lambda')^N \times S_N$, where $S_N = \{\mathbf{v}_i | \sum_{i=1}^N \mathbf{v}_i^2 = N\}$. We shall denote by $X \in \mathcal{S}_N$ a point in the phase space of the system. In these units we took $U = 1$, $R_1 = 0.39$, $R_2 = 0.79$, and Λ is thetorus of side 2[1].

Our main interest is in the SNS of this model system. To be more precise let $\mu_0(dX, N) = \rho_0(X; N)dX$ be an initial measure symmetric in the $\{\mathbf{q}_i, \mathbf{v}_i\}$ and absolutely continuous with respect to the Liouville volume dX projected on $\mathcal{S}_N$. The time evolved measure $\mu_t(dX, \mathbf{E}; N)$ is still absolutely continuous with respect to the Liouville measure with density $\rho_t(X, \mathbf{E}; N)$ for any fixed time t. The SNS is expected to be described by an SRB measure $\mu^+(dX, \mathbf{E}; N)$, given by the weak limit, as $t \longrightarrow \infty$, of $\mu_t(dX, \mathbf{E}; N)$, when it exists. This limit measure is in general not absolutely continuous with respect to the Liouville measure, due to the phase space volume contraction [5], [6]. The existence of such a limit was proven, for $N = 1$ and $|\mathbf{E}| \in [0, E_0]$ (E_0 small) in [3], but no such result is available for $N \geq 2$, because of the lack of uniform hyperbolicity for the zero field system. On the other hand our computer simulations of the dynamics, for N ranging from 1 to 50 and E from 0.04 to 1.0, strongly support the belief that there exists a unique limiting measure $\mu^+(dX, \mathbf{E}; N)$ up to quite large values of $|\mathbf{E}|$, say $|\mathbf{E}| = E \leq 1$. We expect however that the projection of $\mu^+(dX, \mathbf{E}; N)$ on the one particle phase space $\Lambda' \times \Omega_{(N)}$, where $\Omega_{(N)}$ is the ball $|\mathbf{v}| \leq \sqrt{N}$, will yield a one particle density $f^+(\mathbf{q}, \mathbf{v}, \mathbf{E}; N)$ absolutely continuous with respect to $d\mathbf{q}d\mathbf{v}$; this is proven, for instance, for coupled Arnold's cat maps [7]).

To obtain information about f^+ we considered first the case of weak fields. It is tempting to think that for $E \longrightarrow 0$ the singular set on which μ^+ is concentrated will be spread out more or less uniformly on $\mathcal{S}_N$ so that μ^+ will approach weakly the microcanonical measure on the energy surface $\mathcal{S}_N$: this measure is certainly invariant for the dynamics at $E = 0$. If this were the case then $f^+(\mathbf{q}, \mathbf{v}, \mathbf{E}; N)$ would approach, as $E \to 0$, the equilibrium one particle density obtained from the projection of the microcanonical measure: for large N this would be close to the Maxwellian distribution with unit variance [2]. We ran computer simulations for values of the field between 0.04 and 0.12 and $N = 2, 5$ and 50. In all cases we found a one particle distribution that is far from the projection of the microcanonical distribution. Furthermore this distribution appeared to have only very slight dependence on E for those values of the field; so it appears that there is a well defined limit of $f^+(\mathbf{q}, \mathbf{v}, \mathbf{E}; N)$ as $E \to 0$, and that this limit is *not* the projection of the microcanonical measure: there are correlations between the velocities of the particles induced by the field, beyond those corresponding to the energy constraint, which remain when $E \longrightarrow 0$.

This deviation from the microcanonical distribution is reflected also in the behavior of the average current per particle in the steady state, given by $\mathbf{j}(\mathbf{E}, N) = \int \mathbf{v} f^+(\mathbf{q}, \mathbf{v}, \mathbf{E}; N) d\mathbf{q}d\mathbf{v}$ as $E \to 0$. We studied $\mathbf{j}(\mathbf{E}, N)$

[1] See [1] for an explanation of these values.

[2] Note that for large N the Maxwell distribution is typical for points on the energy surface, *i.e.* the set $\mathcal{B}$ on $\mathcal{S}_N$ for which f^+ is not a Maxwellian has measure 0 (w.r.t. dX). Of course since μ^+ is singular w.r.t. dX this need not to be the case here.

numerically as a function of $\mathbf{E}$ and N, see Fig.2 and Fig.3. In the following we will always assume that the electric field is along the positive x-axis, $\mathbf{E} = E\mathbf{1}_x$. This implies that the y component of $\mathbf{j}(\mathbf{E}, N)$ is zero for symmetry reason. We will denote the x component of the current by $j(E, N)$ and call $\kappa(E, N) = j(E, N)/E$ the conductivity. The dependence on N for $E \to 0$ should be given by the Green-Kubo formula for the zero field conductivity when the dynamics of the particles are independent. A straightforward computation then shows that the zero field conductivity of the N particles is:

$$\kappa(0, N) = C_N(0)\kappa(0, 1) \tag{1.3}$$

with $\kappa(0, 1)$ given by the diffusion constant of Bunimovich and Sinai [8] and

$$C_N(0) = \int \frac{1}{|\mathbf{v}|} f^+(\mathbf{q}, \mathbf{v}, 0; N) d\mathbf{q} d\mathbf{v} \tag{1.4}$$

For the microcanonical distribution we easily find:

$$C_N(0) = \sqrt{\pi}\left(1 - \frac{3}{8N} + O\left(N^{-2}\right)\right) \tag{1.5}$$

which is inconsistent with our data although the form of the dependence on N appear to be similar, see sect. 2.1.

Let us consider now the behavior of our model system in the limit $N \to \infty$. As the particles interact only through their average velocity $\mathbf{J}(X(t))$ it seems reasonable to expect that, for $N \to \infty$, $\mathbf{J}$ will stop fluctuating, *i.e.* that for "well behaved" initial distributions [9], [10], [11]

$$\mathbf{J}(X(t)) \longrightarrow \mathbf{j}_t = \int \mathbf{v} f_t(\mathbf{v}, \mathbf{E}) d\mathbf{v} \tag{1.6}$$

where $f_t(\mathbf{v}, \mathbf{E}) = \lim_{N \longrightarrow \infty} f_t(\mathbf{v}, \mathbf{E}; N)$. If this were true in a sufficiently strong sense it would lead to an autonomous Vlasov type equation [9], [10], [11] for f_t where $\dot{\mathbf{v}}$ would be computed self consistently from the (irreversible) dynamics [3]

$$\dot{\mathbf{v}} = \mathbf{E} - \lambda(t)\mathbf{v} + \mathbf{F}_{obs}(\mathbf{q}) \tag{1.7}$$

with $\lambda(t) = \mathbf{E} \cdot \mathbf{j}_t$. The difficulty with proving this behavior, as compared to the [9] case, is that trajectory $X(t)$ and thus also $\mathbf{J}(X(t))$ is not smooth for finite t. The problems are compounded when we consider the $t \longrightarrow \infty$ limit corresponding to the SNS.

Based on numerical evidence we nevertheless believe that

$$\lim_{N \to \infty} f^+(\mathbf{v}, \mathbf{E}; N) = \hat{f}^+(\mathbf{v}, \mathbf{E}) \equiv \lim_{t \to \infty} \hat{f}_t(\mathbf{v}, \mathbf{E}) \tag{1.8}$$

where $\hat{f}_t(\mathbf{v}, \mathbf{E})$ is the solution of the Vlasov equation with a force given by the right hand side of (1.7), and we define for a given function g

$$g(\mathbf{v}) = \int_{\Lambda'} g(\mathbf{q}, \mathbf{v}) d\mathbf{q} \ .$$

The integration over $\mathbf{q}$ is necessary, or at least desirable, since we expect the $t \to \infty$ limit of $\hat{f}_t(\mathbf{q}, \mathbf{v}, \mathbf{E})$ to be singular with respect to $d\mathbf{q}d\mathbf{v}$ as is the $N = 1$ reversible system (1.1). Its projection on the velocity is however expected to be absolutely continuous with respect to $d\mathbf{v}$ [3][7] . Eq(1.8) is thus a form of the law of large numbers which should hold for smooth $\rho_0(X, \mathbf{E}; N)$. Something like this was in fact proven by Ruelle for the stationary state under some hypotheses on the thermostatted dynamics [12]. To make contact with Ruelle's theorem it is convenient to think of Λ_N as a torus of length $2LN$ along the y-axis (perpendicular to $\mathbf{E}$) and length $2L$ along the x-axis. This does not change the dynamics.

To get some analytical handle on the form of the reduced distributions in the SNS we investigated a model system in which the deterministic collisions with the obstacles are replaced by a stochastic process in which particle velocities get their orientations changed at random times, independent for each particle. This yields a

[3] The dynamics (1.1) is reversible in the sense that if $T_t X$ is a solution then $T_t R T_t X = RX$, where R reverses all velocities.

Markov process which replaces the continuity equation for $\rho_t(X,E;N)$ by a linear Boltzmann-like equation, see [13]. We can write either of these equations in the symbolic form:

$$\frac{\partial}{\partial t}\rho_t(\mathbf{Q},\mathbf{V}) + \sum_i \frac{\partial}{\partial \mathbf{q}_i}\{\mathbf{v}_i\rho_t(\mathbf{Q},\mathbf{V})\} + \sum_i \frac{\partial}{\partial \mathbf{v}_i}\{[\mathbf{E}-\alpha(\mathbf{V})\mathbf{v}_i]\,\rho_t(\mathbf{Q},\mathbf{V})\} = \left(\frac{\partial \rho_t}{\partial t}\right)_{\text{coll}}, \tag{1.9}$$

where we have set $X = (\mathbf{Q},\mathbf{V})$ (and dropped the explicit dependence on $\mathbf{E}$ and N). The term on the right hand $\left(\frac{\partial\rho_t}{\partial t}\right)_{\text{coll}}$ represents either the effect of deterministic collisions with the obstacles as given by (1.1) or a collision operator independent of $\mathbf{Q}$, see (3.1). A similar ansatz for the irreversible dynamics (1.7) leads to a Boltzmann-Vlasov equation for the one particle distribution. These equations can be solved analytically as a power series in E and/or numerically. This is described in sect. 3.

In sect. 4 we compare some of the moments, including the current, of the deterministic distribution $f^+(\mathbf{v},\mathbf{E};N)$ with those of the stochastic one. We find surprisingly good agreement once the mean free path appearing in the Boltzmann-like equations is properly interpreted, see sec. 4.2. We note however that a direct computation of the distribution of free paths in the dynamical system (1.1) shows that it is far from being exponential, which is the basic assumption of the Markov process. We therefore have no real explanation for the observed good agreement. We only note that some features of the stationary state appear rather robust with respect to the collision processes with the "obstacles", yielding similar results for different distributions for the free path. In sect. 5 we discuss some general questions about the relation between this thermostatted model and the Drude model of electrical conduction in metals [14].

2. Numerical results

Eq. (1.1) can be solved in terms of quadratures between collisions with the obstacles so the simulation consists mainly in computing the times of successive collisions. At each collision there is an instantaneous change in the velocity of the colliding particle and consequently also in the current $\mathbf{J}$ and thus in the thermostatted force acting on each particle. Assuming that the system is ergodic we can obtain information about the SNS from time averages over a single trajectory. In practice we used a few initial states and found a behavior consistent with this assumption. The relative simplicity of the dynamics enabled us to get fairly accurate results even for 50 particles with relatively small computing power. Our simulation were carried out on a Pentium PC. Error bars are computed by doubling the range of the fluctuations of the time average over the interval $[0.9T, T]$ where T is the total number of collisions computed. After the change of variables described after (1.2) all quantities appearing in the graphs are adimensional.

2.1. The current

Let $\mathbf{j}(\mathbf{E},N)$ be the average current in the steady state μ^+,

$$\mathbf{j}(\mathbf{E},N) = \langle \mathbf{J}\rangle_{\mu^+} = \int \mathbf{v} f^+(\mathbf{v},\mathbf{E},N)d\mathbf{v}\ . \tag{2.1}$$

with $\mathbf{J}$ defined in (1.2). As already noted, in all our computations the electric field is along the positive x-axis, $\mathbf{E} = E\mathbf{1_x}$, all densities are normalized and $j(E,N)$ is the x-component of the current defined in eq.(2.1).

In Fig.2 we plot the conductivity $\kappa(E,N) = j(E,N)/E$ as a function of the field for different numbers of particles, N=1,2,10,15,20,30 and 50. The averages were computed by running simulations in which the total number of collisions with the obstacles varied from 10^9 for $N=1$ to 10^8 for $N=50$.

We note that for very small fields the interaction among the particles is very small so that the invariant distribution is reached only after a very long transient time.

Furthermore, although the current goes to 0 as $E\to 0$, the fluctuations in the current are almost independent of E so that longer and longer simulations are required in order to distinguish the average from the fluctuations when $E\to 0$. For $N = 2,5$ and 10 we checked whether $\frac{d\kappa(E,N)}{dE} \to 0$ as $E\to 0$, as required by the symmetry of the problem if $\kappa(E,N)$ is differentiable at 0. While the results are not definitive they are consistent with such behavior.

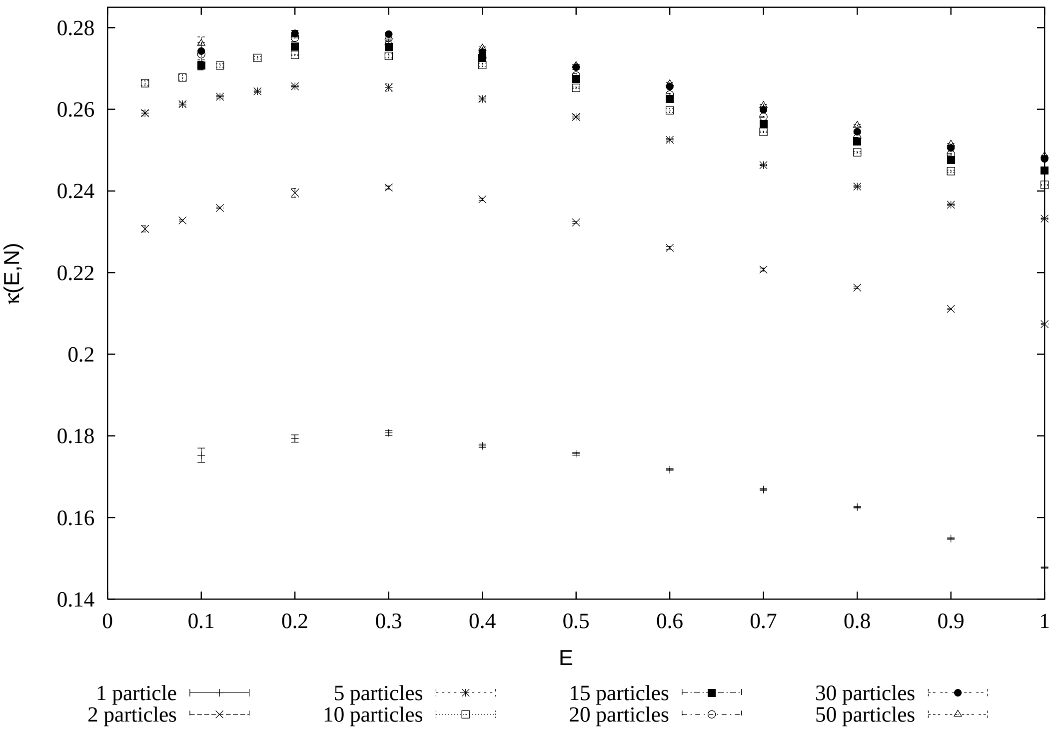

Fig. 2: Conductivity $\kappa(E, N)$ as a function of E for different N.

In Fig. 3 we plot the conductivity as a function of $1/N$ for a few selected values of the field. As can be seen there the behavior of $\kappa(E, N)$ can be well fitted for $N > 2$ by the following formula which is the analogous of eq. (1.3) with $C_N(0)$ given by (1.5) for $E \neq 0$: $\kappa(E, N) = \tilde{\kappa}(E) + c/N$ with $\tilde{\kappa}(E) = \lim_{N\to\infty} \kappa(E, N)$ and c independent from E, at least within the accuracy of our computation. (The value of $\kappa(E, 1)$ is about 15-20% lower than that given by the formula, depending on E). For $E = 0.04$ we have the value of the conductivity for $N = 2, 5$ and 50 as well as the distribution $f^+(\mathbf{v}, E; N)$. We can therefore check directly eq.(1.4) for $E \neq 0$. Fig. 3 contains both the values obtained directly and those obtained from eq.(1.4) for $E = 0.04$. The agreement is clearly very good. Finally plotted in Fig.3 is the value of the conductivity at zero field obtained from eq.(1.5), *i.e.* assuming that the invariant distribution is microcanonical. Although this assumption is inconsistent with the actual numerical data, the behavior is qualitatively similar.

The smoothness, or rather the lack of smoothness, of the current as a function of E for $N = 1$ was extensively discussed in [1] and related there to the discontinuities of the collision map. The data we have for $N \geq 2$ are insufficient to address this question. However it is expected that the stationary current will be smoother than it is in the one particle case, since it is averaged over all particles.

2.2. Distribution functions

To study the space independent part of the one particle density function, $f^+(\mathbf{v}, E; N)$, it is convenient to switch to the variables $r = |\mathbf{v}| \in [0, \sqrt{N}]$ and $\theta \in [-\pi, \pi]$ the angle between the velocity $\mathbf{v}$ and the x-axis. Expanding $f^+(\mathbf{v}, E, N)$ in a Fourier series in θ, we have

$$f^+(\mathbf{v}, E; N) = \sum_{k=0}^{\infty} \psi_k(r, E; N) \cos k\theta \ , \tag{2.2}$$

where only terms in $\cos k\theta$ appear due to the symmetry of the problem. Note that $2\pi r \psi_0(r, E; N)$ is the stationary probability density for the modulus of $\mathbf{v}$ while

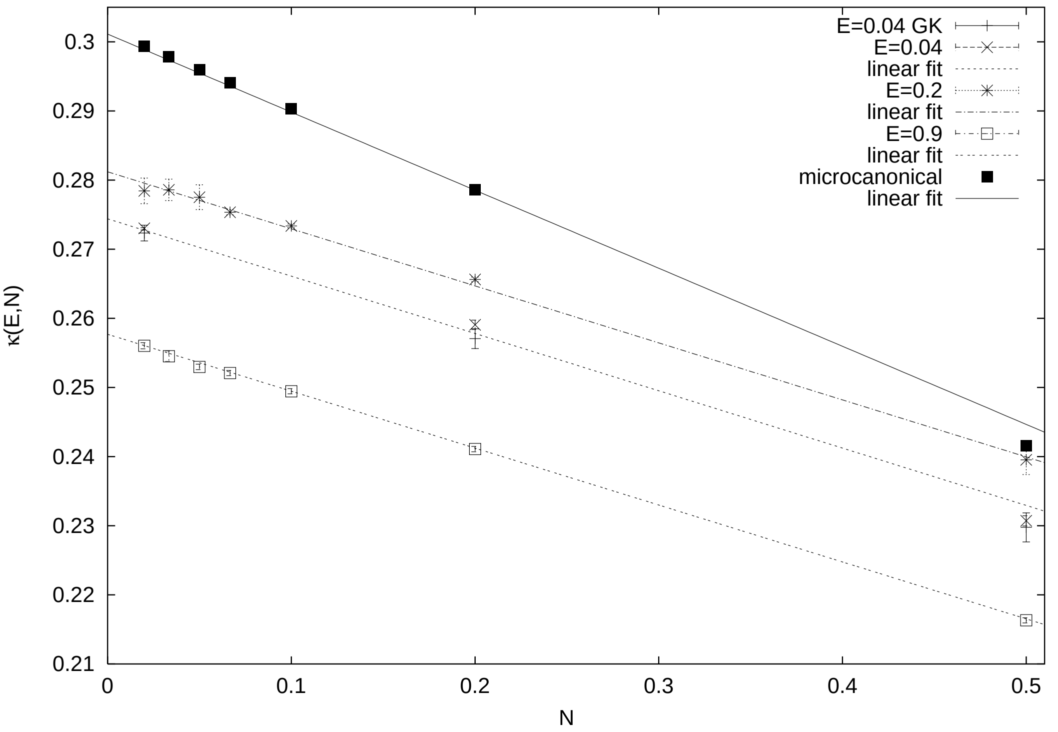

Fig. 3: $\kappa(E,N)$ as a function of N^{-1} for different E. Also plotted is the conductivity obtained from eq.(1.3) using the actual distribution function, see next section, for $E = 0.04$ and compared with the value obtained by a direct simulation at the same field. Finally the highest line represents the conductivity obtained from eq.(1.3) using a microcanonical hypothesis.

$$j(E,N) = \pi \int_0^{\sqrt{N}} dr\, r^2 \psi_1(r,E;N) \ . \tag{2.3}$$

In Fig. 4 we plot $2\pi r\psi_0(r,E;2)$ for $E = 0.04, 0.08, 0.12$ while Fig. 5 is a plot of $\pi r\psi_1(r,E;2)/E$ for the same values of the field. Both appear to be almost independent of E for those values of E so we believe that Figs. 4 and 5 represent a good approximation for the limiting behavior $E \to 0$. Observe that, due to the symmetry $E \to -E$ we expect the corrections to these functions to be of $O(E^2)$. For comparison we also plotted there the results obtained analytically from the stochastic model discussed in the Introduction and in section 3.

In Fig. 4 we also plot the " microcanonical" density of $|\mathbf{v}_1|$ obtained from the microcanonical ensemble of 2 particles with $\mathbf{v}_1^2 + \mathbf{v}_2^2 = 2$. The microcanonical one particle density $f_{\rm micro}(\mathbf{v})$ is of course isotropic and the speed distribution, $2\pi|\mathbf{v}_1|f_m(|\mathbf{v}_1|, E=0;2)$, is

$$2\pi|\mathbf{v}_1|f_m(|\mathbf{v}_1|, E=0;2) = \frac{1}{\pi}|\mathbf{v}_1| \int \delta(\mathbf{v}_1^2 + \mathbf{v}_2^2 - 2)d\mathbf{v}_2 = |\mathbf{v}_1| \ \mathcal{H}(2 - \mathbf{v}_1^2) \ , \tag{2.4}$$

where $\mathcal{H}(x)$ is the Heaviside function. This is seen to be very different from what we obtain from our simulations or analytically from the stochastic model for $E \to 0$. We did a similar analysis for $N > 2$ and in Figs. 6 and 7 we present the corresponding results for $N = 50$.

2.3. The $N = \infty$ limit

As discussed in sec. 2.1, $\kappa(E,N) \to \tilde{\kappa}(E)$ as $N \to \infty$. We compared the $\tilde{\kappa}(E)$ obtained from our simulation, see Fig. 3, with that obtained from the irreversible eq.(1.7). A way to do this self-consistently would be to choose the parameter λ in eq.(1.7) such that

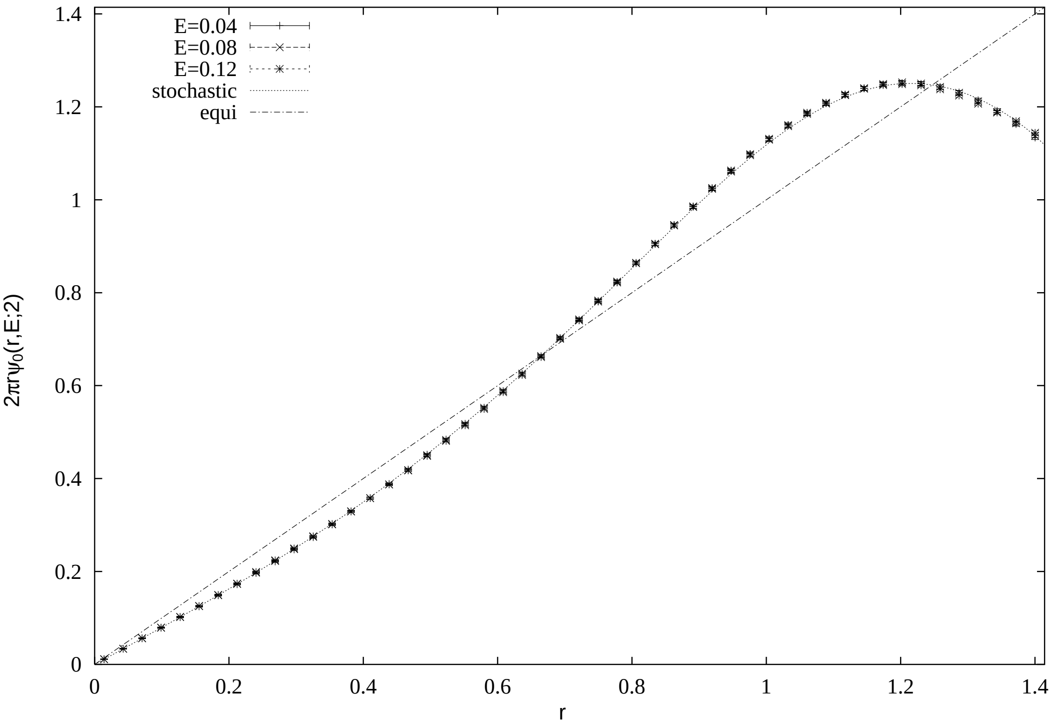

Fig. 4: Plot of $2\pi r\psi_0(r,E;2)$ for different values of E. The straight dashed line is obtained from the microcanonical distribution, Eq.(2.4). The dotted line gives the result for the stochastic model

$$\hat{U}(E) = \int d\mathbf{v}|\mathbf{v}|^2 \hat{f}^+(\mathbf{v},E) = 1$$

and show that for this value of λ the conductivity $\hat{\kappa}(E)$ for the system described by eq.(1.7) is equal to $\tilde{\kappa}(E)$. Rather than doing this, we took the $\tilde{\kappa}(E)$ deduced from the simulations as in Fig.3 and used it to determine λ, i.e. we set $\lambda = \tilde{\kappa}(E)E^2$ in eq.(1.7). We then computed, via simulation of eq.(1.7), a new conductivity $\hat{\kappa}(E)$. In Fig.8 we compare $\hat{\kappa}(E)$ and $\tilde{\kappa}(E)$. The agreement is very good. We observe that it follows from eq.(1.7)that $E^2\hat{\kappa}(E)/\hat{U}(E) = \lambda$ so that this agreement also confirms the self-consistency discussed above.

As for the reversible dynamics we can write

$$\hat{f}^+(\mathbf{v},E) = \sum_{k=0}^{\infty} \phi_k(r,E)\cos k\theta \tag{2.5}$$

In Figs. 6 and 7 we compare $2\pi r\psi_0(r,E;50)$ and $\pi r\psi_1(r,E;50)$ with $2\pi r\phi_0(r,E)$ and $\pi r\phi_1(r,E)$ respectively. The agreement is very good. As we did for $N=2$ in Fig. 4 and Fig. 5 we also plotted in Figs. 6 and 7 the results obtained analytically from the stochastic model discussed in the Introduction and in section 3. In Fig. 6 we also plot the microcanonical density, *i.e.* a Maxwellian with $< \mathbf{v}_1^2 >= 1$.

3. Thermostatted Stochastic Evolution

We now describe more precisely the stochastic model system in which the collisions between particles and obstacles are replaced by independent random scattering events. The model is specified by writing the right hand side of eq. (1.9), the evolution equation for the N-particle phase space density of our system, which we now call $F_t(\mathbf{Q},\mathbf{V})$, to distinguish it from the mechanical $\rho_t(\mathbf{Q},\mathbf{V})$, as

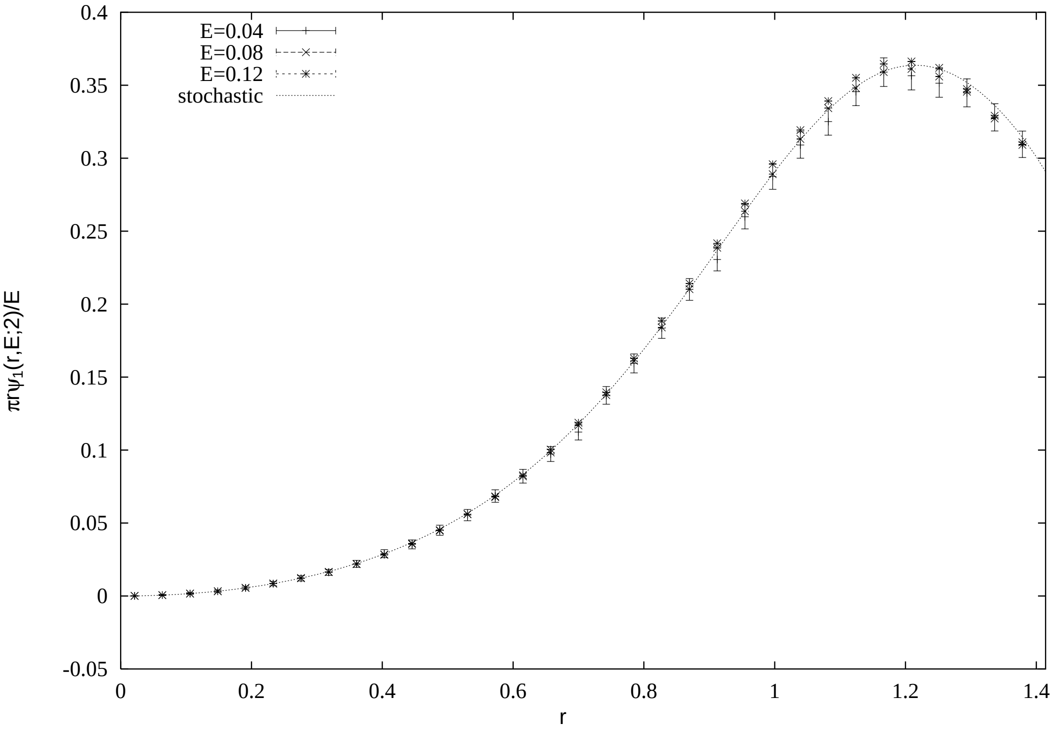

Fig. 5: Plot of $\pi r\psi_1(r,E;2)/E$ for different values of E. The dotted line gives the result for the stochastic model

$$\left(\frac{\partial F(\mathbf{Q},\mathbf{V},\mathbf{E})}{\partial t}\right)_{\rm coll} = l^{-1}\sum_{i=1}^{N}\int_{(\mathbf{n}\cdot\mathbf{v}_i)<0}\frac{(\mathbf{v}_i'\cdot\mathbf{n})}{2}\left(F(\mathbf{Q},\mathbf{V}_i',\mathbf{E})-F(\mathbf{Q},\mathbf{V},\mathbf{E})\right)d\mathbf{n} \tag{3.1}$$

In (3.1) $\mathbf{n}$ is a unit vector in the direction of the momentum transfer in a "collision", $|\mathbf{n}|=1$, $\mathbf{v}'=\mathbf{v}-2\mathbf{n}(\mathbf{n}\cdot\mathbf{v}_i)$ and $\mathbf{V}_i'$ is identical to $\mathbf{V}_i$ except for its i-th component which is replaced by $\mathbf{v}_i'$. The coefficient l^{-1} multiplying the collision term is the inverse of the mean free path between collisions, a parameter to be specified.

Eq. (1.9) together with (3.1) describes a Markov process in which particles change the directions of their velocities as if they were undergoing independent random collisions with "phantom obstacles" at a rate equal to $l^{-1}|\mathbf{v}|$ with a uniformly distributed impact parameter [15]. Between collisions the particles move according to eq.(1.1). This model can be thought of as, and presumably even proven to be, the Boltzmann-Grad limit of our system: *i.e.* , we place discs of radius R randomly in a square of side L with density ρ and then take $R\to 0$, $\rho\to\infty$ such that $l=\frac{1}{2\rho R}$ stays constant, see [16].

This system will, like our mechanical system, eq.(1.1), conserve energy, so setting $\sum\mathbf{v}_i^2=N$ the evolution takes place on $\mathcal{S}_N$. By general arguments [17], [18] we expect that this system will, for $E\neq 0$ approach, as $t\to\infty$, a unique stationary density $F(\mathbf{V},\mathbf{E};N)$ which will satisfy the equation

$$\sum_{i=1}^{N}\frac{\partial}{\partial\mathbf{v}_i}\left\{[\mathbf{E}-\mathbf{E}\cdot\mathbf{J}\mathbf{v}_i]\,F(\mathbf{V},\mathbf{E};N)\right\} = \left(\frac{\partial F(\mathbf{V},\mathbf{E};N)}{\partial t}\right)_{\rm coll} \tag{3.2}$$

For small E we expand $F(\mathbf{V},\mathbf{E};N)$ as a formal power series in $\mathbf{E}$:

$$F(\mathbf{V},\mathbf{E};N)=F(\mathbf{R},\Theta)=\sum_{n=0}^{\infty}E^nF^{(n)}(\mathbf{R},\Theta) \tag{3.3}$$

where we have set $\mathbf{v}_i=(r_i\cos\theta_i,r_i\sin\theta_i)$ and $\mathbf{R}=(r_1,\ldots,r_N)$, $\sum_i r_i^2=N$, $\Theta=(\theta_1,\ldots,\theta_N)$. Observe that in this way we get a singular perturbation problem because E multiplies the highest order derivative in eq.(3.2).

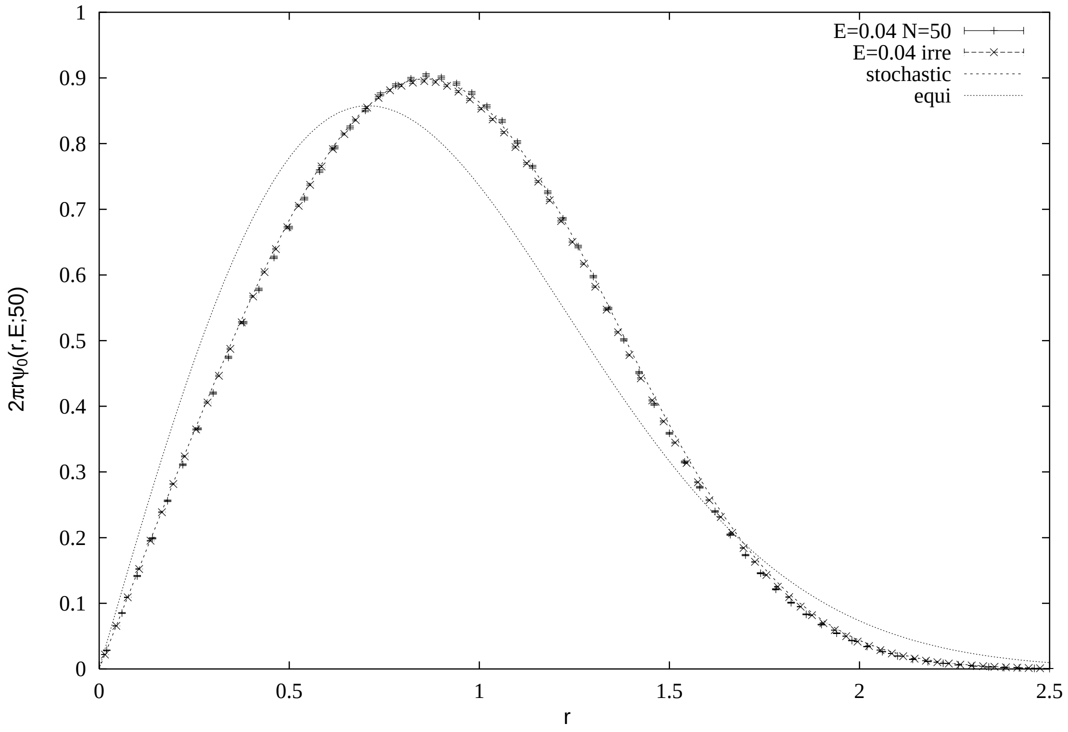

Fig. 6: Plot of $2\pi r\psi_0(r, E; 50)$ for $E = 0.04$. Also shown are the results from simulations of (1.7) and from analytic solutions of the corresponding stochastic equation, Eq.(3.10). For comparison we also show the microcanonical result, corresponding to a Maxwellian.

Moreover $F^+(\mathbf{V}, \mathbf{E}; N)$ clearly depends only on E/l so that we can, for the time being, set $l = 1$. Finally we can write, as in the previous section,

$$F^{(n)}(\mathbf{R}, \Theta) = \sum_{\mathbf{k}\in\mathbb{Z}_+^N} F^{(n)}(\mathbf{R}, \mathbf{k}) \prod_{i=1}^{N} \cos(k_i\theta_i) \tag{3.4}$$

where we have again used the symmetries of the problem.

Substituting (3.4) into (3.3) one gets a hierarchy of equations linking $F^{(n)}(\mathbf{R}, \mathbf{k})$ to $F^{(n-1)}(\mathbf{R}, \mathbf{k}^i)$ where $\mathbf{k}^i = (k_1, \ldots, k_i + 1, \ldots, k_N)$. From this, and from the fact that the kernel of the collision operator depends only on $\mathbf{R}$ we get that $F^{(n)}(\mathbf{R}, \mathbf{k}) = 0$ if $|\mathbf{k}| > n$. $F^{(0)}(\mathbf{R}, 0)$ satisfies the relation:

$$\frac{\partial}{\partial r_i} F^{(0)}(\mathbf{R}, 0) = \frac{4}{3} r_i F^{(1)}(\mathbf{R}, 0^i) \tag{3.5}$$

while for $F^{(1)}(\mathbf{R}, 0^i)$ we get the equation

$$\sum_i \left\{ \left(-\frac{r_i}{U} - \frac{1}{r_i} \right) F^{(1)}(\mathbf{R}, 0^i) + \frac{\partial}{\partial r_i} F^{(1)}(\mathbf{R}, 0^i) \right\} = 0 \tag{3.6}$$

with $U = \sum_i r_i^2$. Equations (3.5) and (3.6) are easily solved and, together with the fact that $F^{(1)}(\mathbf{R}, 0) \equiv 0$ give us $F(\mathbf{R}, \Theta)$ to first order in E

$$F(\mathbf{R}, \Theta) = C\delta(\sum_{i=1}^{N} r_i^2 - N) \left[\frac{1}{(\sum_i r_i^3)^{\frac{2N-1}{3}}} + \frac{3(2N-1)E}{4} \frac{r_i \cos\theta_i}{(\sum_i r_i^3)^{\frac{2N+2}{3}}} + O(E^2) \right] \tag{3.7}$$

where C is a normalization constant. It is possible to write out the full hierarchy of equations for $F^{(n)}(\mathbf{R}, \mathbf{k})$ and see that they can be solved iteratively but it is not clear that this is useful. We shall therefore use eq.(3.7)

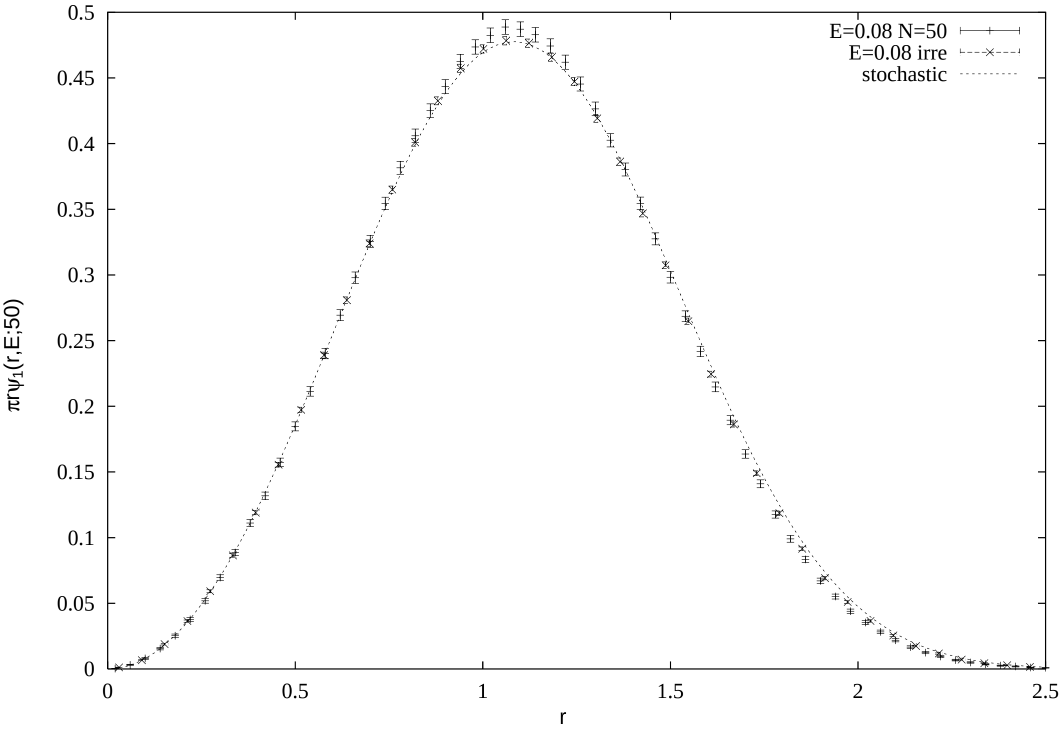

Fig. 7: Plot of $\pi r\psi_1(r,E;50)/E$ and comparison with stochastic irreversible dynamics for $E = 0.08$

to compare with our numerical data for small values of E. To do so we define the one particle distribution $\tilde{f}(\mathbf{v}, E; N)$ and develop it in a Fourier series exactly as in eq.(2.2):

$$\tilde{f}(\mathbf{v}, E; N) = \int d\mathbf{v}_2 \cdots d\mathbf{v}_N \tilde{F}(\mathbf{V}, E; N) = \sum_{k=0}^{\infty} \tilde{\psi}_k(r, E; N) cos(k_i\theta_i) \tag{3.8}$$

Before doing any comparisons we consider the stochastic version of the $f_i(\mathbf{v}, E)$ obtained from the irreversible dynamics defined by eq.(1.7). Putting $\lambda = E^2\nu$, ν to be set to $\bar{\kappa}(E)$ when compared with the deterministic model, we get

$$\frac{\partial}{\partial \mathbf{v}} \left\{ \left[\mathbf{E} - E^2\nu\mathbf{v}\right] \tilde{f}_i(\mathbf{v}, \mathbf{E}) \right\} = \left(\frac{\partial \tilde{f}_i(\mathbf{v}, \mathbf{E})}{\partial t} \right)_{\text{coll}} \tag{3.9}$$

where the collision term is again given by eq.(3.1) with $N = 1$. Observe that although eq.(3.9) contains three parameter (E, ν and l) it depends only on El and νl^{-1}. Developing $\tilde{f}_i(\mathbf{v}, \mathbf{E})$ in a power series in E we obtain in analogy to (3.7)

$$\tilde{f}_i(\mathbf{v}, \mathbf{E}) = Ce^{-\frac{8}{9l}\nu r^3}(1 + 2\nu Er\cos\theta) + O(E^2) \tag{3.10}$$

where C is a normalization constant.

To compare $\tilde{f}_i(\mathbf{v}, \mathbf{E})$ with the large N limit of $\tilde{f}(\mathbf{v}, \mathbf{E}; N)$ given in (3.8) and (3.9) we need to fix the parameter ν (setting $l = 1$). This can be done self-consistently requiring that:

$$\int |\mathbf{v}|^2 \tilde{f}_i(\mathbf{v}, \mathbf{E}) d\mathbf{v} = 1 \tag{3.11}$$

Solving eq.(3.11) for ν and using it to compute $\tilde{f}_i$ we expect that:

$$\lim_{N\to\infty} \tilde{f}(\mathbf{v}, E; N) = \tilde{f}_i(\mathbf{v}, E) \tag{3.12}$$

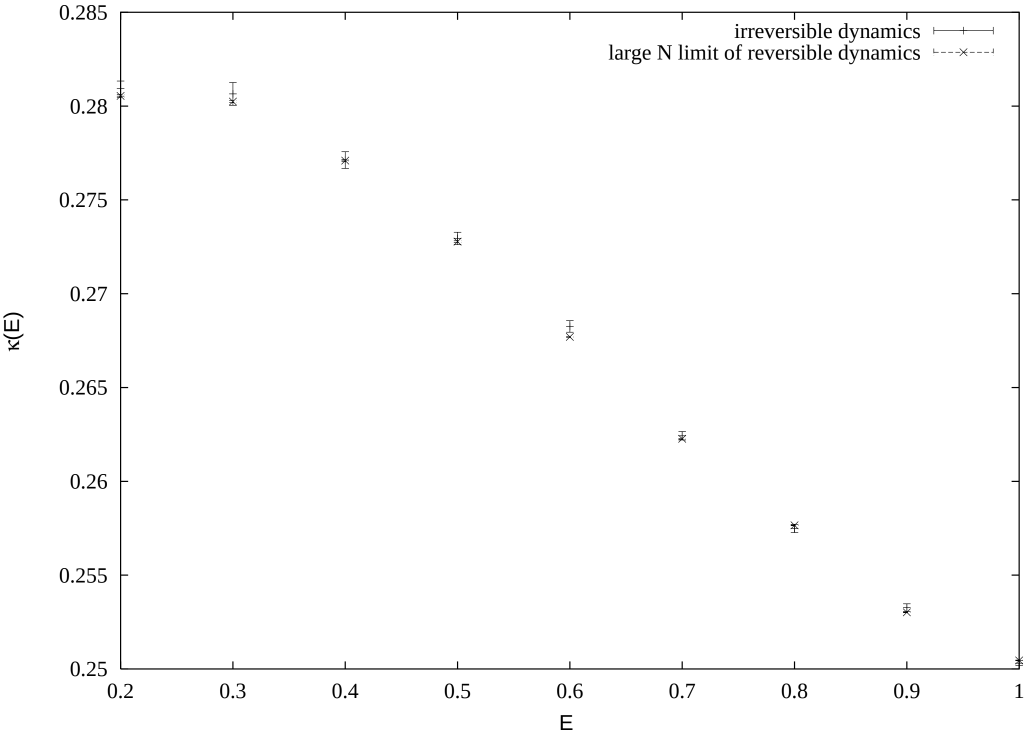

Fig. 8: Comparison between the limiting value of the conductivity $\tilde{\kappa}(E)$ in the reversible model and in the irreversible model $\kappa_\infty(E)$.

While we have not proven this equivalence we believe that it should follow from general considerations: it would follow formally from showing that, in the limit $N \to \infty$, $\tilde{F}(\mathbf{v}, \mathbf{E}; N)$ factorizes, as is usually the case for systems with mean field type interactions. This is certainly consistent with our numerical results.

4. Comparison between the deterministic and stochastic time evolution

4.1. The distribution of the modulus of **v**

For $N = 1$ the exact solution, for $E = 0$, of both the stochastic and mechanical models is $f(\mathbf{v}, 0; 1) = \delta(\mathbf{v}^2 - 1)$. For $N = 2$, we are able to compute the one particle distribution from eq.(3.7). This yields

$$r\tilde{\psi}_0(r, E; 2) = \frac{Cr}{r^3 + (2 - r^2)^{3/2}} + O(E^2) \tag{4.1}$$

where C is a normalization constant. This is plotted in **F**ig. 4 and one can easily see that the agreement with the numerical solution of the deterministic model is very good.

A similar agreement is obtained for $N = 5$ although, as already said we were not able to integrate eq.(3.8) for $N > 2$ so that we computed this integral numerically by simulating the process associated to eq.(1.9) with collision term given by eq.(3.1).

Finally for $N = 50$ we see in Fig. 6 that our deterministic (1.1), stochastic (3.9) and irreversible (1.7) models give indistinguishable results. This certainly suggests the validity of (1.7) and (3.12) for large N.

4.2. The first Fourier component of the distribution of $\mathbf{v}$

The analysis of the first Fourier component of the distribution of $\mathbf{v}$ is less straightforward because we must fit the parameter l appearing in eq.(3.1). In the stochastic system l represent the mean free flight of a particle. The concept of mean free flight is not uniquely defined for the mechanical model. For this reason we used l as a fitting parameter for matching $\tilde{\psi}_1(r, E; N)$ with $\psi_1(r, E; N)$. We will go back to the mechanical meaning of this parameter in the following section. The case $N = 2$ is reported in Fig.5 where, for the periodic case, we used a field $E = 0.04$ and for the stochastic one we have the expression

$$r\tilde{\psi}_1(r, E; 2) = \frac{1}{2}\frac{9El}{4}\frac{Cr^2}{\left(r^3 + (2 - r^2)^{3/2}\right)^2} + O(E^3) \tag{4.2}$$

with C the same costant appearing in eq.(4.1) The agreement is again very good and we obtain from the fit $l = 0.46$ (in the unit discussed in the introduction). As in the previous case we did the same comparison for 5 particles, obtaining again a very good agreement. Moreover also in this case the value of l is very close to that obtained for $N = 2$. Finally it is interesting to check if this agreement remains when $N \to \infty$, *i.e.* for the stochastic irreversible equation (3.9). As can be seen from Fig.7 the agreement is again very good and we still get the same value for the parameter $l \simeq 0.46$.

We were also able to compute $\psi_k(r, E; 2)$ and $\phi_k(r, E)$ for $k = 2$ and 3. It is also easy to compute the lowest order contribution to $\tilde{\psi}_k(r, E; 2)$ and $\tilde{\phi}_k(r, E)$, extending the computation from section 3. It is thus possible to compare, at least in this limited situation, the results. Contrary to what we found for $k = 0$ and 1, $\psi_2(r, E; 2)$ is quite different from $\tilde{\psi}_2(r, E; 2)$. Analogously $\phi_2(r, E)$ and $\tilde{\phi}_2(r, E)$ differ significantly. A comparison of the term with $k = 3$ also shows deviations between the mechanical and the stochastic models although, surprisingly, much smaller than those found for $k = 2$. We note however that for this comparison we only have data for $E = 0.012$.

4.3. The mean free flight.

In kinetic theory one can define the mean free flight in two ways. Denoting by $\ell_i(X)$ the distance travelled by particle i before its first collision with an obstacle starting form the point $X \in \mathcal{S}_N$, l_0 is the average of $\ell_i(X)$ with respect to the SRB distribution $\mu^+(dX, \mathbf{E}; N)$ (it clearly does not depend on i). On the other hand we can consider the set $\mathcal{S}_N^i$ of points such that particle i is undergoing a collision, *i.e.* $\mathbf{q}_i$ is on the boundary of one of the scatterers, then l_1 is the average of $\ell_i(X)$ on $\mathcal{S}_N^i$ with respect to the projection of the SRB distribution $\mu^+(dX, \mathbf{E}; N)$. Observe that for the stochastic model these two quantities are identical.

We computed both l_0 and l_1 for the mechanical system with $N = 2, 5, 50$ and for the irreversible dynamics eq.(1.7) with $E = 0.04$. This was done by running a very long trajectory and taking the average of the distance travelled by a particle between two collisions to compute l_1 or numerically integrating $\ell_i(X)$ along the trajectory to compute l_0. The results appears to be independent of N, at least within the accuracy of our computations, and are:

$$l_0 = 0.46$$
$$l_1 = 0.58$$

The value of l_0 agrees very well with the value obtained from the fit of l reported in the previous section. This implies that the correct way to compare the stochastic and the mechanical model is to use l_0 as the mean free flight parameter in eq.(3.1). This is consistent with the Green-Kubo formula eq.(1.3). We saw in sect. 2.1 that eq.(1.3) is well verified for the conductivity at small field of the deterministic model. In the case of the stochastic model eq.(1.3) reduces to an integral relation between $F^{(0)}(\mathbf{R}, 0)$ and $F^{(0)}(\mathbf{R}, 0^i)$, see eq.(3.5)(3.6) in sect. 3. We did not prove this identity although numerical analysis for small N seems to verify it. Finally the agreement between $\psi_0(r, 0; N)$ and $\tilde{\psi}_0(r, 0; N)$ observed in sect.4.1 tells us that the ratio between the conductivity for the deterministic and stochastic dynamics is independent of N at least for $E \to 0$. From eq.(3.7) we know that the conductivity for the stochastic model with one particle and $E = 0$ is $3l/4$ so that also for the deterministic model we have

$$\kappa(0, 1) = \frac{3}{4}l_0 \tag{4.3}$$

This relation is also very well verified by our computation for the 1 particle system.

To better compare the deterministic and stochastic models we also computed the distribution $P(\ell, \mathbf{E}; N)$ of $\ell_i(X)$ with respect to the SRB distribution. This distribution for 5 particles and $E = 0.04$ is shown in Fig.9 together with an exponential law with the same average, *i.e.* the distribution one would obtain running the same simulation for the stochastic case. We did similar computation for $E = 0.04$ and $N = 2, 10$ and 50. The results are again independent from N.

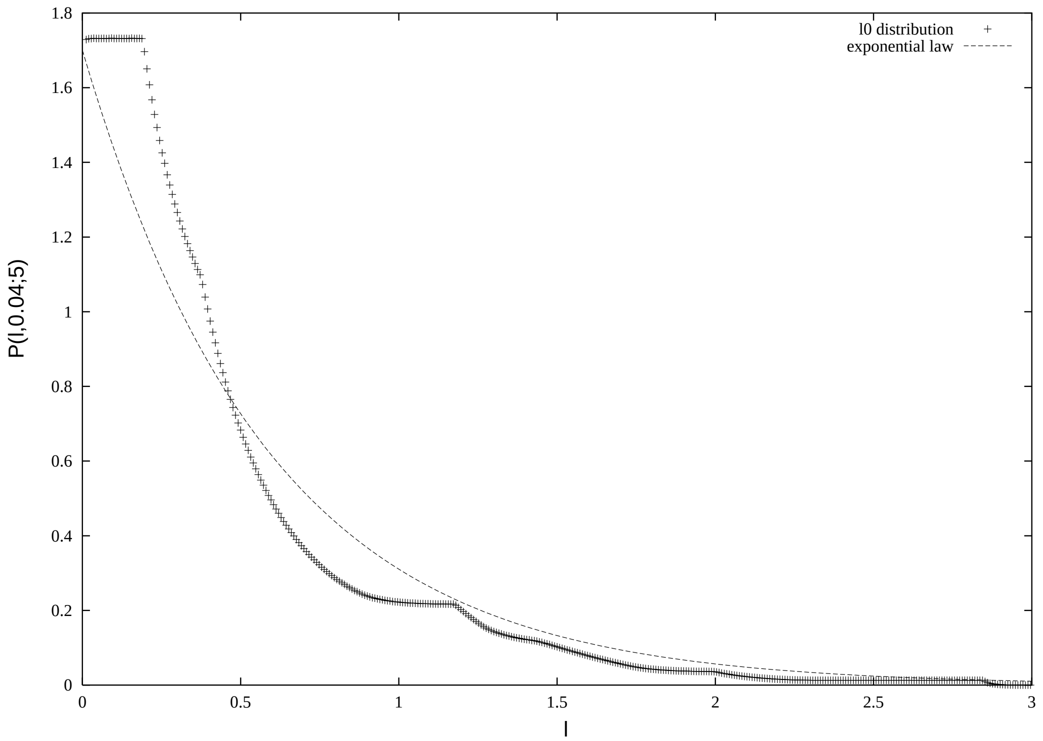

Fig. 9: Free path distribution $P(l, 0.04; 5)$ compared with an exponential distribution with the same average

5. Conclusions

To put our study here in a physical context we note that a system of noninteracting electrons moving under the influence of an external electric field while undergoing elastic scatterings is often used as a crude model of electrical conduction in metals (the Drude model) [19],[20],[14]. To obtain the conductivity the velocity distribution function of the electrons is then computed from a Boltzmann type equation like eq.(3.2): with $N = 1$ and *without* the thermostatting $\mathbf{E} \cdot \mathbf{J}$ term. By doing this calculation only to linear order in E one avoids the problem that, without the thermostat eq.(3.2) does not have a solution since the system will never be in a true steady state [21]. A crucial ingredient in the calculation is the explicit assumption that for $E = 0$ the distribution is one corresponding to equilibrium at a given specified temperature T, *i.e.* Maxwellian for a classical system.

This description of the system of independent electrons interacting with the lattice of ions only via elastic collision is clearly not realistic. It is just used for obtaining a simple quick answer for the zero (small) field conductivity. For a more complete description of the steady state in a conductor one has to consider the system to be in contact with some *reservoir* which will absorb the heat generated by the current. It is this interaction with some external reservoir that was replaced, in the model considered here, by an artificial thermostat. To our surprise however we found that this modeling does not lead to a Maxwellian distribution when $E \to 0$ even when N is very large. This means that there is no *equivalence of ensembles* when it comes to modeling how the energy is extracted from the system- at least when there is no direct interactions between the particles other than that induced by the thermostat. We expect (and have some indication [22]) that this will change when we include collisions between the particles. Still it raises some caution about "thermostats" as a model for the description of stationary nonequilibrium states.

Acknowledgment. We are indebted to G. Gallavotti, P.L. Garrido, S. Goldstein, A. Rohlenko, D. Ruelle and particularly H. van Beijeren for many helpful discussions and suggestions. Much of the research was carried out at Rutgers University where it was supported in part by NSF Grant DMR-9813268, and Air Force Grant F49620-98-1-0207. D. D. is Chargé de recherches at the FNRS. V. R. was supported by the Foundation BLANCEFLOR Boncompagni-Ludovisi née Bildt.

References.

[1] F. Bonetto, D. Daems, J.L. Lebowitz, *Properties of Stationary Nonequilibrium States in the Thermostatted Periodic Lorentz Gas I: the One Particle System*, Journ. Stat. Phys. **101**, 35-60 (2000)

[2] Moran Hoover, *Diffusion in a periodic Lorentz gas*, Journ. Stat. Phys. **48**, 709–726 (1987).

[3] N.I. Chernov, G.L. Eyink, J.L. Lebowitz, Ya.G. Sinai, *Steady state electric conduction in the periodic Lorentz gas*, Commun. Math. Phys. **154**, 569–601 (1993).

[4] F. Bonetto, G. Gallavotti, P.L. Garrido, *Chaotic principle: an experimental test*, Physica D **105**, 226–252 (1997).

[5] J.M. Eckmann, D. Ruelle, *Ergodic Theory of Chaos and Strange Attractors*, Rev. Mod. Phys. **57** 617–656 (1985).

[6] D. Ruelle, *Smooth dynamics and new theoretical ideas in nonequilibrium statistical mechanics*, Journ. Stat. Phys. **95**, 393–468 (1999)

[7] F. Bonetto, A.J. Kupiainen, J.L. Lebowitz, *Perturbation theory for coupled Arnold cat maps: absolute continuity of marginal distribution*, preprint.

[8] L. Bunimovich, Ya. Sinai, *Statistical properties of Lorentz gas with periodic configuration of scatterers*, Commun. Math. Phys. **78**, 479–497 (1980)

[9] W. Braun, K. Hepp, *The Vlasov dynamics and its fluctuations in the $\frac{1}{N}$ limit of interacting classical particles* , Commun. Math. Phys. **56**, 101-113 (1977)

[10] O.E. Lanford, *Time dependents phenomena in statistical mechanics*, Mathematical Problems in theoretical physics (Proc. Internat. Conf. Math. Phys., Lausanne, 1979), 103-118

[11] H. Spohn, *Large scale dynamics of interacting particles*, Spinger Verlag (1991)

[12] D. Ruelle, *A remark on the equivalence of isokinetic and isoenergetic thermostats in the thermodynamic limit*, Journ. Stat. Phys. **100**, 757–763 (2000)

[13] H. van Beijeren, J. R. Dorfman, E. G. D. Cohen, H. A. Posch, and Ch. Dellago, *Lyapunov Exponents from Kinetic Theory for a Dilute, Field-Driven Lorentz Gas*, Phys. Rev. Lett. **77** 1974–1977 (1996)

[14] H. Lorentz, *Collected Papers*, Martinus Nijhoff, The Hague, 1936

[15] C. Cercignani, *The Boltzmann equation and its applications*, Springer-Verlag, New York (1988)

[16] G. Gallavotti, *Rigorous theory of the Boltzmann equation in the Lorentz gas*, Nota Interna n.358, Istituto di Fisica, Università di Roma, 10 feb. 1972

[17] S. Goldstein, J. Lebowitz, E. Presutti, *Mechanical systems with stochastic boundaries*, Proceedings of conference on random fields, 403–419,Esztergom, Hungary, June 1979, Coll. Math. Soc. János Bolyai

[18] S. Goldstein, J. Lebowitz, E. Presutti, *Stationary Markov chains*, Proceedings of conference on random fields, 421–461,Esztergom, Hungary, June 1979, Coll. Math. Soc. János Bolyai

[19] N.W. Ashcroft, N.D. Mermin, *Solid States Physics*, Holt, Rinehart and Winston, New York (1976)

[20] C. Kittel: *Introduction to Solid States Physics*, Wiley, New York (1986)

[21] J. Piasecki, E. Wajnryb, *Long-Time Behavior of the Lorentz Electron Gas in a Constant, Uniform Electric Field*, Journ. Stat. Phys. **21**, 549–559 (1979).

[22] G. Garrido, Private communication